Bulletin of Earthquake Engineering (2006) 4:249–273
DOI 10.1007/s10518-006-9009-y

Modelling Seismic Hazard in Earthquake Loss Models with Spatially Distributed Exposure

HELEN CROWLEY[1] and JULIAN J. BOMMER[2,*]
[1]*European School for Advanced Studies in Reduction of Seismic Risk (ROSE School); c/o EUCENTRE, Via Ferrata 1, Pavia 27100, Italy;* [2]*Department of Civil and Environmental Engineering, Imperial College London, SW7 2AZ, UK*
[*]*Corresponding author. Tel.: +44-20-75945984, Fax: +44-20-75945934, E-mail: j.bommer@imperial.ac.uk*

Received 25 August 2005; accepted 12 February 2006 / Published online: 1 April 2006

Abstract. The prediction of possible future losses from earthquakes, which in many cases affect structures that are spatially distributed over a wide area, is of importance to national authorities, local governments, and the insurance and reinsurance industries. Generally, it is necessary to estimate the effects of many, or even all, potential earthquake scenarios that could impact upon these urban areas. In such cases, the purpose of the loss calculations is to estimate the annual frequency of exceedance (or the return period) of different levels of loss due to earthquakes: so-called loss exceedance curves. An attractive option for generating loss exceedance curves is to perform independent probabilistic seismic hazard assessment calculations at several locations simultaneously and to combine the losses at each site for each annual frequency of exceedance. An alternative method involves the use of multiple earthquake scenarios to generate ground motions at all sites of interest, defined through Monte–Carlo simulations based on the seismicity model. The latter procedure is conceptually sounder but considerably more time-consuming. Both procedures are applied to a case study loss model and the loss exceedance curves and average annual losses are compared to ascertain the influence of using a more theoretically robust, though computationally intensive, procedure to represent the seismic hazard in loss modelling.

Key words: average annual loss, earthquake loss modelling, ground-motion variability, scenario earthquakes, seismic hazard, spatial correlation

1. Introduction

Earthquake loss modelling is an area of growing importance, driven to a large degree by the needs of the insurance and reinsurance industries but also with application to emergency planning and also to seismic code drafting committees (Bommer *et al.*, 2005). All of the inputs to an earthquake loss model have large associated uncertainties, and the identification, quantification and incorporation of these uncertainties into the calculations form an integral part of establishing a loss model. Equally important is to develop an understanding of how these uncertainties impact on the results

of the loss estimation. Crowley *et al.* (2005) performed a systematic analysis of the impact of epistemic uncertainties in the ground motion and vulnerability elements of a model for estimating losses from a single earthquake scenario, concluding that the parameters with the greatest impact are those related to the seismic resistance of the exposed building stock. This paper extends that earlier study by calculating losses – using a single set of vulnerability parameters – from multiple earthquake scenarios in order to estimate loss rates. In a companion paper (Bommer and Crowley, 2006) the specific issue of the way the aleatory variability in the ground-motion prediction equation can be included in the loss calculations, and the consequences of using the different options, is examined in detail.

The same region used for the sensitivity study by Crowley *et al.* (2005), located to the north of the Sea of Marmara in Turkey (Figure 1) has been chosen as a test case for this study because of the high levels of hazard and exposure in this area, and also to take advantage of the previous data collection and experience in earthquake loss modelling in this area (Bommer *et al.*, 2002). The reader is referred to Crowley *et al.* (2005) for more information on the assumptions made in the loss model used herein. An important issue, which should be highlighted here is that the study presented in this paper should not be considered as a definitive loss model for the Marmara region and the results are presented for comparative purposes only.

Only reinforced concrete buildings are considered in the case study loss model presented herein, the structural characteristics of which are discussed

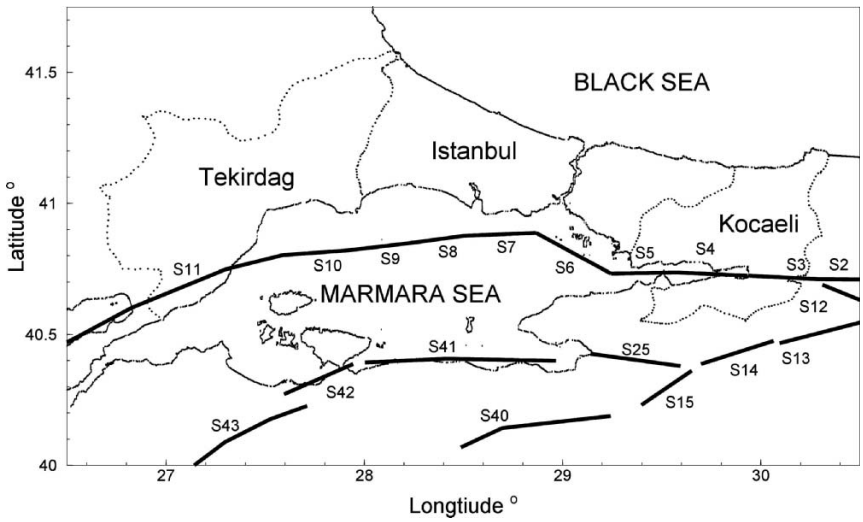

Figure 1. Location of study area showing boundaries of the provinces of Kocaeli, Istanbul and Tekirdag, and the fault segmentation model proposed by Erdik *et al.* (2004).

in detail in Crowley *et al*. (2005). The vulnerability of these buildings is predicted using the DBELA method, which models the seismic demand and the structural capacity in terms of displacements (Crowley *et al*., 2004). The uncertainty in the displacement capacity (that arises when a group of buildings, which may have different geometrical and material properties, is considered together) and the displacement demand is modelled using the first-order reliability method (FORM). In the applications in this paper, the variability in the earthquake demand is removed from the reliability calculations since it is necessarily included in the seismic hazard model (Bommer and Crowley, 2006).

It is important to state that the DBELA vulnerability methodology is in continuous development and is used herein because of the advantages it offers of computational efficiency. The results, however, must not be taken to be indicative of actual expected losses in the Marmara region. The vulnerability procedure currently models the buildings as single bare frames, whereas in fact they are three dimensional structures with infill panels; the inclusion of these factors into the methodology is part of ongoing research. The losses calculated using the current formulation are almost definitely overestimated; an earlier study by Spence *et al*. (2003), although not based on DBELA, concluded that observed losses in this region due to the 1999 Kocaeli earthquake may have been overestimated as a result of underestimating the contribution of infill panels to seismic resistance. However, since the loss results obtained in this paper and in the earlier study by Crowley *et al*. (2005) are only used for comparative purposes, this limitation is not important.

A probabilistic seismic hazard assessment for the Marmara Region has been carried out and stochastic earthquake catalogues have also been generated using the procedure discussed in Section 2.5. A FORTRAN program has been coded to produce the stochastic earthquake catalogues, whilst the program EZ-FRISK Version 4.1 (Risk Engineering Inc., 1998) has been used to carry out the probabilistic seismic hazard assessment (PSHA). The data regarding the tectonics and seismicity of the region required for both of these hazard assessments are described below.

Erdik *et al*. (2004) describe the tectonic regime of the Marmara Sea region and the work of many researchers to develop tectonic models using low-resolution bathymetric data and the occurrences of earthquakes. The western portion of the North Anatolian Fault zone (NAFZ) dominates the tectonic regime of the Marmara Sea area: the NAFZ manifests as a single fault line east of 31.5°E whereas to the west it splays into a complex fault system (Figure 1). Erdik *et al*. (2004) have used many published findings regarding the fault system below the Sea of Marmara (e.g. Pinar, 1943; Ergun and Ozel, 1995; Le Pichon *et al*., 1999) to develop a fault segmentation model (Figure 1). The most significant tectonic element in the

region is the Main Marmara fault: a through-going dextral strike-slip fault system.

The study area for the PSHA is confined to 39.5° – 42°N, 25.8° – 33.5°E. The background seismicity is assumed to include all earthquakes of $5.5 < M_w < 7.0$. All earthquakes greater than $M_w = 7$ are assumed to occur on faults through characteristic earthquakes, and the fault segmentation model proposed by Erdik *et al.* (2004) has been used to model the location of these characteristic earthquakes (Figure 1). The GSHAP catalogue (www.seismo.ethz.ch/gshap/turkey) has been used to model the historical and instrumental seismicity of the Marmara region. The catalogue is comprised of events of $M_w \geq 5.5$; the data of earthquakes of $M_w \geq 5.5$ are assumed to be complete from 1900. The removal of fore- and after-shocks was not considered necessary as these are rarely of magnitude ≥ 5.5. The Gutenberg–Richter recurrence relationship has been calculated using maximum likelihood regression for the sources of background seismicity using the events of magnitude $5.5 < M_w < 7.0$ from 1900 until 1999 from the earthquake catalogue using the program Wizmap (http://www.quakes.bgs.ac.uk/hazard/wizmap.htm). The *b*-value was calculated for the whole area due to a lack of data in some zones and was found to be 0.69; this was then fixed for each zone and the *a*-value was calculated accordingly.

The characteristic magnitudes of the fault segments have been determined using the empirical relationship between magnitude, sub-surface rupture length and rupture area for strike-slip faults (Wells and Coppersmith, 1994). The historical seismicity, the tectonic models and the known slip rates along the faults were the main data used by Erdik *et al.* (2004) to assign recurrence intervals to the fault segments (from which the annual rates of occurrence are calculated, as shown in Table 1). All faults are assumed to be strike-slip with a dip of 90° and the minimum magnitude has been taken as the characteristic magnitude minus 0.1 units and the maximum magnitude was assumed to be the characteristic magnitude plus 0.1 units.

Although the use of a time-dependent stochastic model would lead to a more rigorous assessment of the probabilistic hazard, when characteristic fault models are used, the influence of the recurrence model on the PSHA of the Marmara region is outside the scope of this study, and the Poisson model is used herein. Furthermore, the aim of this paper is to compare the loss results when two different procedures are used to represent the seismic hazard and so provided the same assumptions are made for both methods, the use of the Poisson model as opposed to time-dependent models should not influence the conclusions made herein.

The ground-motion prediction equations of Boore *et al.* (1997) have been used in this study to produce displacement spectra using the same

Table I. Poisson model characteristic earthquake parameters associated with fault segments shown in Figure 1 (from Erdik *et al.*, 2004)

Fault segment	Characteristic Magnitude (M_w)	Annual rate of occurrence	Fault segment	Characteristic Magnitude (M_w)	Annual rate of occurrence
S2	7.2	0.0071	S12	7.2	0.0040
S3	7.2	0.0071	S13	7.2	0.0017
S4	7.2	0.0071	S14	7.2	0.0017
S5	7.2	0.0057	S15	7.2	0.0010
S6	7.2	0.0048	S25	7.2	0.0010
S7	7.2	0.0040	S40	7.2	0.0010
S8	7.2	0.0040	S41	7.2	0.0010
S9	7.2	0.0050	S42	7.2	0.0010
S10	7.2	0.0050	S43	7.2	0.0010
S11	7.5	0.0067			

methodology and assumptions as applied in the sensitivity study of the Marmara region carried out by the authors (Crowley *et al.*, 2005). In HAZUS and the NEHRP guidelines (FEMA, 2004), a constant displacement plateau is taken to commence at a period T_{VD} (T_L in NEHRP), given by the following equation:

$$T_{VD} = 10^{\frac{M_W - 5}{2}} \tag{1}$$

In FEMA 366 (FEMA, 2001) the corner period is taken to be constant for spectra derived from the hazard curves and it is assumed to be 10 s, which corresponds to an earthquake of magnitude 7. This assumption is necessary with the use of PSHA because all of the earthquakes have been aggregated to attain the hazard curve and thus the corner period cannot be modified with magnitude. In the loss exceedance curves obtained herein a corner period of 12.6 s, corresponding to a magnitude of 7.2, has been assumed considering that the majority of the fault segments have this characteristic magnitude (Table 1).

To obtain response spectra for damping levels higher than 5% (which are necessary given the equivalent linearization approach in the vulnerability assessment procedure), the response spectra are reduced using the spectral ratio equation in EC8 (CEN, 2003):

$$\eta = \sqrt{\frac{10}{5+\xi}} \tag{2}$$

Bommer and Mendis (2005) have shown that current reduction factors used to modify the 5% response spectrum for higher levels of damping should in fact be dependent on the duration of the ground motion, which is related to the distance and magnitude of the earthquake. Spectral ratios (the ratio between the spectral ordinate of a given equivalent viscous damping level and that at 5%) for ground-motion prediction equations can easily be calculated at various distances and magnitudes. Regression analysis can then be used to produce relationships between the spectral ratio and the viscous damping ratio, magnitude and distance. When scenario earthquakes are used in loss calculations, the spectral ratio can thus be modified for each magnitude-distance pair, whilst when a PSHA-based approach is applied, a constant spectral ratio has to be used throughout.

2. Modelling seismicity for loss assessment

In this section, different options for modelling earthquake occurrences in a loss estimation model are considered. In each case, the resulting ground motions will be calculated using a ground-motion prediction (attenuation) equation, which will inevitably have a large associated scatter that is generally represented by the standard deviation of the logarithmic residuals, which are assumed to follow a normal distribution. The influence of this scatter in the ground motion is discussed in detail in the companion paper by Bommer and Crowley (2006). Since in this paper the purpose is to calculate loss rates, the aleatory variability in the ground motion is necessarily removed from the vulnerability calculations and included directly in the estimation of the seismic demand.

2.1. SINGLE EARTHQUAKE SCENARIOS

For the communication of seismic risk to the general public, or for emergency planning purposes, the estimation of the impact on the built environment from a single scenario, such as the repetition of a significant historical earthquake, can be very useful. In fact, many loss assessment studies have adopted a deterministic approach using a single event or a small set of earthquake scenarios (e.g. Cardona and Yamin, 1997; Faccioli *et al.*, 1999; Tantala *et al.*, 2002). In general, the scenario earthquakes are determined by studying the historical destructive earthquakes that have occurred in the region and identifying their sources; repetitions of these earthquakes are then adopted as the damage scenarios in the loss study.

Nevertheless, for most decision-making processes such as those within the insurance and reinsurance industry and in seismic code draft committees, the prediction of the effects of all possible future events is necessary. In this case the purpose of the loss calculations is to estimate the

annual frequency of exceedance (or the return period) of different levels of loss due to earthquakes: so-called loss exceedance curves. Loss exceedance curves can also be used to calculate the annual average loss (AAL), which is the expected value of a loss probability distribution; the AAL is particularly important for the insurance industry as it can be used to set annual premiums. In the following sections, various possibilities are presented for modelling the ground motions from all future events such that loss exceedence curves can be generated.

2.2. PROBABILISTIC SEISMIC HAZARD ANALYSIS

A straightforward option for representing the demand in a loss model (when ground motions with a range of return periods need to be simultaneously defined at multiple sites) is to first perform a PSHA for each site and then convolve the hazard curves at each site with the exposure and vulnerability of the building stock; finally, the losses at each site are combined at each return period. Conventional PSHA was not, however, derived for this purpose and so its use in loss modelling has recently been called into question (e.g. Chang *et al.*, 2000; Rhoades and McVerry, 2001; Taylor *et al.*, 2001; Leonard and Steinberg, 2002). Nevertheless, this approach was proposed, for example, by Cao *et al.* (1999), wherein the shaking was represented in the form of macroseismic intensity, and it was also employed in FEMA 366 (FEMA, 2001) to calculate the annual estimated loss (equivalent to the AAL) for each county in the USA. Campbell *et al.* (2000a, b) have also proposed PSHA models for use in loss estimation and risk management in the United States and Japan.

The main problem with using conventional PSHA for the derivation of loss curves for spatially distributed exposure is that the ground-motion variability, which has a large spatial (inter-event or station-to-station) component, is implicitly assumed to be entirely temporal (intra-event or earthquake-to-earthquake), which consequently leads to overestimation of the seismic demand on the exposed building stock (Bommer and Crowley, 2006).

Nevertheless, PSHA hazard curves can be used when a single site is being considered in the loss model because there is no need to produce a correlated random field of ground motions, as will be illustrated in the case study presented herein. The use of PSHA hazard curves in the generation of loss exceedance curves is described in detail in Section 3.1.

2.3. DISAGGREGATED SCENARIO EARTHQUAKES FROM PSHA

Disaggregation of PSHA results is a process, which allows the identification of individual earthquake scenarios that contribute to the hazard for

a given ground-motion parameter at a selected annual frequency of exceedance (e.g. McGuire, 1995; Bazzurro and Cornell, 1999). The proportion of the total hazard caused by different magnitude, distance, number of standard deviations triplets (M–D–ε) defined in ranges of values or bins can be identified and plotted on a 4D plot, which gives the proportion of the total hazard on the vertical axis as a function of the distance and magnitude on the two horizontal axes, whilst the contribution of the scatter ε is plotted as a different colour on the vertical axis, for each M–D bin. For many purposes, the most dominant scenarios can be selected from these disaggregated plots and used to produce realistic response spectra or to select appropriate accelerograms for the design of structures. For earthquake loss assessment, however, all of the scenario earthquakes defined in the plot need to be accounted for, as described below.

The use of disaggregated scenarios in earthquake loss modelling would first require a PSHA of the whole region to be carried out. At each site within the study, and at each annual frequency of exceedance (AFOE) of interest (of which there will most likely be more than 10), the hazard estimate would need to be disaggregated to obtain a plot of M–D–ε. Each scenario in the plot would then be used to produce demand spectra and these would be convolved with the vulnerability, and the loss calculated. The loss obtained for each scenario would then need to be multiplied by the contribution of that scenario to the hazard estimate and then the losses from all scenarios would be integrated. This would then need to be repeated for each AFOE in order to produce a loss exceedance curve; when hundreds of sites are to be considered, the computational effort required to produce loss vs AFOE curves using disaggregated scenarios would most likely render the loss study unfeasible.

2.4. MODIFIED HISTORICAL CATALOGUES

The simulation of earthquake catalogues that are compatible with the seismicity of a given area is one method, which can be used to produce multiple scenario earthquakes for the derivation of loss exceedance curves. The historical catalogue cannot generally be used for the definition of such event sets as it is unlikely to describe the full range of events in time and space that could occur within a specified region.

Bommer *et al*. (2002) modified the historical catalogue to eliminate spatial incompleteness for their Turkish loss model based on multiple earthquake scenarios. A total of 1039 earthquake scenarios were triggered with a minimum magnitude of 5.5; each scenario in the catalogue had an annual frequency of occurrence assigned to it, calculated from the recurrence relationship. A projected fault rupture plane was used as the model of each earthquake event based on the predominant mechanism and average dip

angle for each source zone. For an event of given magnitude, slip type and dip angle, surface fault rupture length and width were calculated from relationships of Wells and Coppersmith (1994). Events were triggered with random epicentral locations: anywhere within a source zone for magnitude < 7 and along a mapped fault of a certain minimum length for magnitude ≥ 7. The estimated length of the fault rupture for a given magnitude defined the selection of available faults within a zone; it was assumed that the rupture would not exceed the mapped fault length. For a given (sub-) zone, multiple events were triggered for a given magnitude and the event annual frequency was calculated by dividing the frequency for that magnitude by the number of events triggered in the (sub-)zone, so as to maintain the temporal description of the seismicity (see Figure 2).

For each event in the modified earthquake catalogue, ground motions at each of the sites in the loss model can be predicted using a ground-motion prediction equation. The location and magnitude of each event can be used in conjunction with the site conditions in a prediction equation to give the median ground-motion parameter of interest.

2.5. STOCHASTIC EARTHQUAKE CATALOGUES USING MONTE–CARLO SIMULATION

The Monte–Carlo simulation method, also known as stochastic modelling, provides a simple and robust method to generate large numbers of synthetic earthquake catalogues or stochastic event sets, which, unlike historical catalogues, are temporally and spatially complete. The use of stochastic catalogues for earthquake loss assessment appears to be common in the commercial sector (e.g. Eugster *et al.*, 1999; Liechti *et al.*, 2000; Zolfaghari, 2000; Windeler *et al.*, 2004).

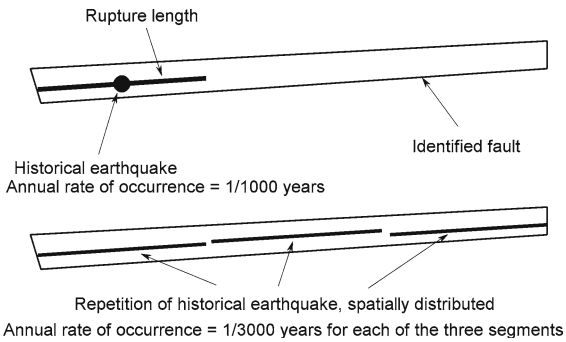

Figure 2. Illustrative diagram showing the modification of historical earthquakes to compensate for spatial incompleteness.

Musson (1998, 1999) has provided an insight into the mechanism of the Monte–Carlo method for the generation of synthetic earthquake catalogues and their use in probabilistic seismic hazard analysis. The basic concept to the Monte–Carlo method is the controlled generation of random numbers from specified probability distributions. A seismic source zone model prepared for a conventional probabilistic seismic hazard analysis describes with a certain degree of completeness the spatial and temporal distribution of earthquakes within a given region. The temporal distribution is modelled using recurrence relationships; in general a Gutenberg–Richter relationship is used for area sources and a characteristic earthquake model is used for active faults. The method described herein assumes a Poisson model, such that the occurrence of earthquakes is independent of the time elapsed since the last event, although time-dependent models can also be used.

For active faults, modelled using a characteristic magnitude recurrence relationship, the procedure to define a stochastic catalogue for each fault segment is as follows:

(i) For each year in the catalogue, a random number between 0 and 1 is generated from a uniform distribution.
(ii) If the random number is less than the annual probability of earthquakes on that fault then this implies an earthquake in that year, otherwise no earthquakes occur.
(iii) The spatial distribution of the earthquakes is already determined from the fault segmentation model and the characteristic magnitude is as defined for that fault segment.

If the whole process is repeated for a very large number of years (e.g. 100,000 years of data), then the ratio between the number of times that the random number falls below the annual rate of earthquakes and the total number of simulations should be equal to the annual probability of earthquakes on the fault.

For distributed seismicity in area sources, a two-step random number process is required to define the catalogue for each source zone:

(i) For each year in the catalogue, a random number, P_{random}, between 0 and 1 is generated from a uniform distribution.
(ii) If the random number is less than the annual probability of events above a chosen minimum magnitude, M_{min}, (i.e. P_{min}, obtained from the annual rate N_{min} by assuming a Poisson model) and greater than the annual probability of events, P_{max}, below a chosen maximum magnitude, M_{max}, then there is an earthquake within the source zone in that year:

$$N_{\min} = 10^{a-bM_{\min}} \tag{3}$$

$$N_{\max} = 10^{a-bM_{\max}} \tag{4}$$

$$P_{\min} = 1 - \exp^{-N_{\min}} \tag{5}$$

$$P_{\max} = 1 - \exp^{-N_{\max}} \tag{6}$$

$$\text{If } P_{\min} > P_{\text{random}} > P_{\max} \rightarrow \text{earthquake} \tag{7}$$

where a and b are calculated for the area source from the earthquake catalogue, using the Gutenberg–Richter relationship.

(iii) When an earthquake is randomly generated, the magnitude is determined using the random number P_{random} and the recurrence relationship:

$$N_{\text{random}} = -\ln(1 - P_{\text{random}}) \tag{8}$$

$$M = \frac{a - \log(N_{\text{random}})}{b} \tag{9}$$

(iv) Each epicentre within the source zone is located by a random latitude and longitude co-ordinate (N°, E°) by generating uniformly distributed numbers within the latitude and longitude bounds of the source. The assumption is thus that any location within the source zone has an equal probability of being the epicentre of the next earthquake, though this does not have to be the case and other assumptions can be incorporated into the model.

Once a synthetic earthquake catalogue of sufficient length has been generated, then for each earthquake generated, the ground shaking at each site can be simulated using a ground-motion prediction equation and the associated aleatory variability in the equation.

For each earthquake generated:

(i) A random number is sampled from the standard normal probability distribution to obtain a random number of standard deviations (ε): this represents the number of inter-event standard deviations, $\varepsilon_{\text{inter}}$, which is multiplied by the inter-event logarithmic standard deviation in the ground-motion parameter (σ_{inter}).

(ii) A ground-motion prediction equation is used to calculate the logarithmic mean value of the ground shaking parameter (e.g. the spectral ordinate at a given period) at the site using the magnitude and distance from source to site.

(iii) At each site, a second random draw from the standard normal probability distribution is made to define the number of intra-event standard deviations, $\varepsilon_{\text{intra}}$, which is multiplied by the intra-event logarithmic standard deviation in the ground-motion parameter (σ_{intra}).

It would be possible to include the spatial correlation between the ground motions at different sites here, though at the expense of greatly increasing the computational effort (e.g. Bommer and Crowley, 2006).

(iv) The two random measures of logarithmic scatter are then added to the logarithmic mean of the ground-motion parameter and the exponential is taken to find the predicted ground motion at each site.

Of the three procedures presented in Section 2 for generating earthquake catalogues and associated ground motions at multiple sites, the use of Monte–Carlo simulation is the only procedure, which is theoretically robust in terms of the representation of the aleatory variability; furthermore, the ground motions produced using Monte–Carlo simulation as described herein, have the same annual frequency of exceedance as those from PSHA hazard curves.

2.6. COMPARISON OF HAZARD ESTIMATES

A hazard map depicting the peak ground acceleration (PGA) with a return period of 2500 years at each of the 150 municipalities in the three provinces of Kocaeli, Istanbul and Tekirdag is presented in Figure 3. This hazard map has been compared with an equivalent map produced by Erdik *et al.* (2004) in their PSHA study of the Marmara Region, and the two give consistent results, with slightly higher PGA values predicted by Erdik *et al.* (2004) in some areas, mainly due to the fact that the map was plotted using NEHRP B/C boundary site conditions, compared to the site class B used in this study.

Hazard curves for the spectral acceleration at 2 s – using the Boore *et al.* (1997) ground-motion prediction equation with local site effects modelled using representative V_{s30} values – for three of the 150 municipalities (indicated in Figure 3) are presented in Figure 4: Gölcük is assigned to NEHRP site class D, based on the findings of Spence *et al.* (2003), and Saray and Adalar are assigned to site class C (as inferred from a geological map of the region). The consideration of three sites in the loss calculations presented herein is sufficient for illustrative purposes and these particular sites have been chosen due to their large geographical separation and distinct levels of hazard.

An earthquake catalogue for the Marmara region spanning 100,000 years with approximately 50,000 scenario earthquakes has been generated using Monte–Carlo simulation and the ground motions at each of the three sites have been estimated using the Boore *et al.* (1997) ground-motion prediction equations along with the random generation of an inter-event variability for each earthquake and an intra-event variability for each site, as described in Section 2.5. The ground motions from all of the simulations

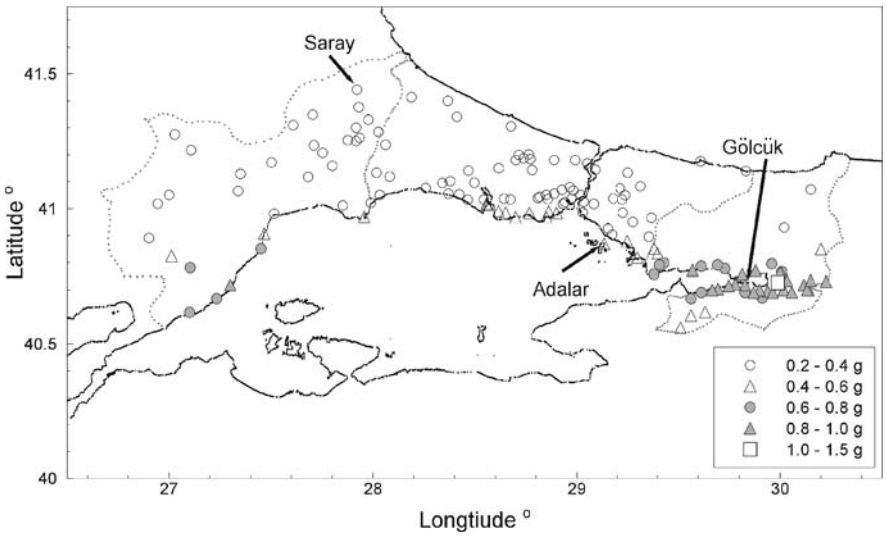

Figure 3. The PGA at all municipalities for NEHRP B (rock) site class for a return period of 2500 years with the location indicated for the three municipalities of Gölcük, Adalar and Saray.

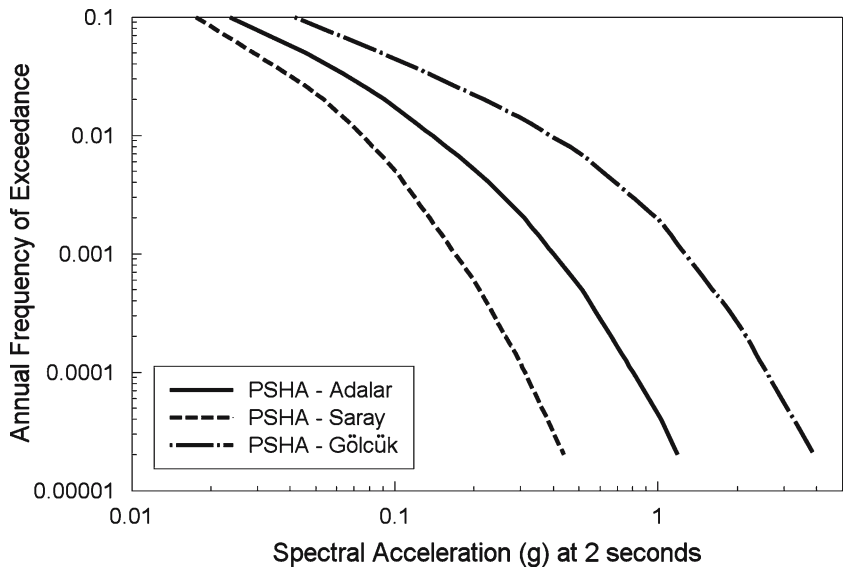

Figure 4. Hazard curves for three sites in the Marmara region from conventional PSHA.

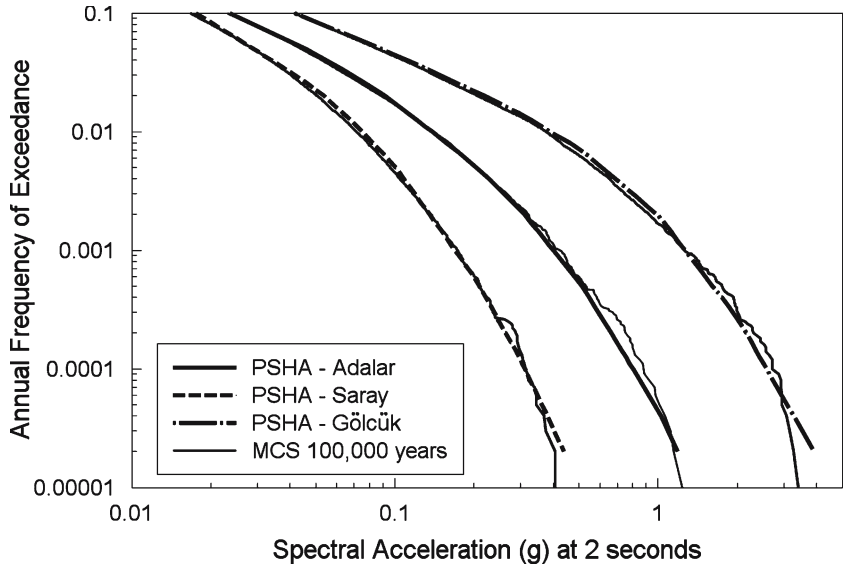

Figure 5. Comparison of hazard curves for spectral acceleration at 2 s using conventional PSHA and by generating a synthetic catalogue of 100,000 yrs with MCS.

have been sorted by size from the largest to the smallest for each of the sites separately and thus hazard curves have been produced for each site (Figure 5) and compared with those from conventional PSHA.

It can be observed that the accuracy of the hazard curves generated from Monte–Carlo simulation diminishes at very low-AFOE. In the Monte–Carlo method, probabilities are not calculated analytically and so very low exceedance frequencies may not be accurately represented in the stochastic catalogues sampled; however, provided a large number of simulations are performed, this potential disadvantage can be overcome. Hence, in order to study the sensitivity of these curves to the number of simulations, an earthquake catalogue for the region has been generated with a length of 500,000 years (containing approximately 250,000 scenario earthquakes) and hazard curves have again been produced (Figure 6).

The accuracy at low AFOE is significantly improved in Figure 6, though it could be further improved by an even longer earthquake catalogue. However, the benefit of producing accurate ground motions at low AFOE needs to be weighed against the additional computational effort, especially considering that once a mean damage ratio (MDR: the ratio of the cost of repair to the cost of replacement) of 1 has been attained at a given AFOE, calculations at lower AFOE no longer need to be carried out. The sensitivity of the loss curves to the length of the catalogue is studied further in Section 3.2.

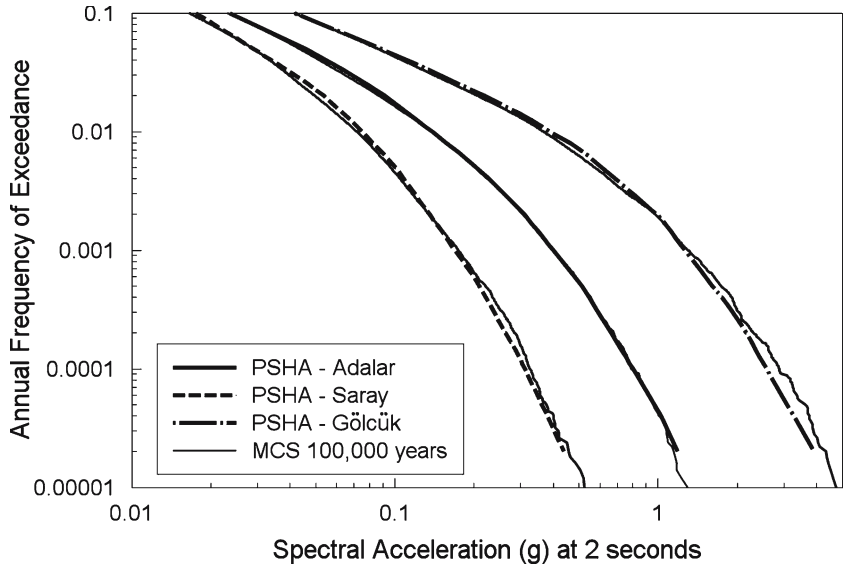

Figure 6. Comparison of hazard curves for spectral acceleration at 2 s using conventional PSHA and by generating a synthetic catalogue of 500,000 yrs with MCS.

3. Calculation of loss curves

In Section 2, the procedures for generating ground motions at multiple sites for a range of annual frequencies of exceedance using PSHA and Monte–Carlo Simulation (MCS) have been presented. In this section, the two procedures are applied to a case study loss model and the loss exceedance curves and AAL values that are predicted for the two methods are compared with the objective of determining the error in using the theoretically flawed, though computationallyefficient, method of PSHA-derived hazard curves. Hence, these results are specifically for comparative purposes and should not be taken as loss results for the Marmara Region.

3.1. PSHA-based loss calculations

The procedure documented in FEMA 366 (FEMA, 2001) to produce a combined loss exceedance curve, and subsequently the AAL, at a collection of sites has been adapted to allow the use of the DBELA vulnerability methodology, as described in what follows.

(i) Produce hazard curves of AFOE (λ) of spectral acceleration for various periods of vibrations at each site by carrying out a PSHA with the site conditions accounted for in the ground-motion prediction equation.

At each site:

(ii) Choose a number of return periods (=1/AFOE) at which the loss calculations will be carried out (e.g. 10, 50, 100 years etc.).

(iii) For each return period, obtain the spectral acceleration at each response period from the hazard curves.

(iv) The acceleration spectra are transformed into displacement spectra via the pseudo-spectral relationships.

(v) The displacement spectrum should be extrapolated past 2 s up to a corner period, T_{VD}, taken as 12.6 s as discussed in Section 1 (see Crowley *et al.*, 2005 for more details).

(vi) For each building class (e.g. 3-storey, reinforced concrete, beam-sway frame), the probability of failing each limit state is calculated using the DBELA methodology (Crowley *et al.*, 2004), and these probabilities are used to calculate the proportion of buildings in each damage band (slight, moderate, extensive or complete).

(vii) The mean damage ratio (MDR) is calculated by assigning damage ratios to the proportion of buildings in each damage band and integrating the results.

(viii) The MDR values at all sites are summed for each AFOE.

(ix) A plot of AFOE vs combined MDR can now be produced and once rebuilding costs for each building type have been defined, the MDR can be directly transformed into loss. The AFOE can be transformed into an annual probability of exceedance (q) by assuming, for example, a Poisson model:

$$q = 1 - e^{-\lambda} \tag{10}$$

(x) The AAL can be computed by calculating the expected value of the loss probability curve.

Following the FEMA 366 (FEMA, 2001) procedure, 37 return periods between 10 and 50,000 years at which to calculate the loss have been selected. FEMA 366 suggests that eight return periods are sufficient (100, 250, 500, 750, 1000, 1500, 2000 and 2500 years), following a sensitivity study that compared the stability of the loss results to the number of return periods for 10 metropolitan regions using 5, 8, 12, 15 and 20 return periods. However, it is stated that more return periods, especially those lower than 100 years, may be required for more seismically active regions, such as California. A large number of return periods have been selected herein to study the required number of return periods for this loss model.

The loss exceedance curves for the three sites that have been calculated using the procedure of FEMA 366 are presented in Figure 7. The weighing factors used for the MDR calculations are those suggested in HAZUS: 2% for slight damage, 10% for moderate damage, 50% for extensive damage

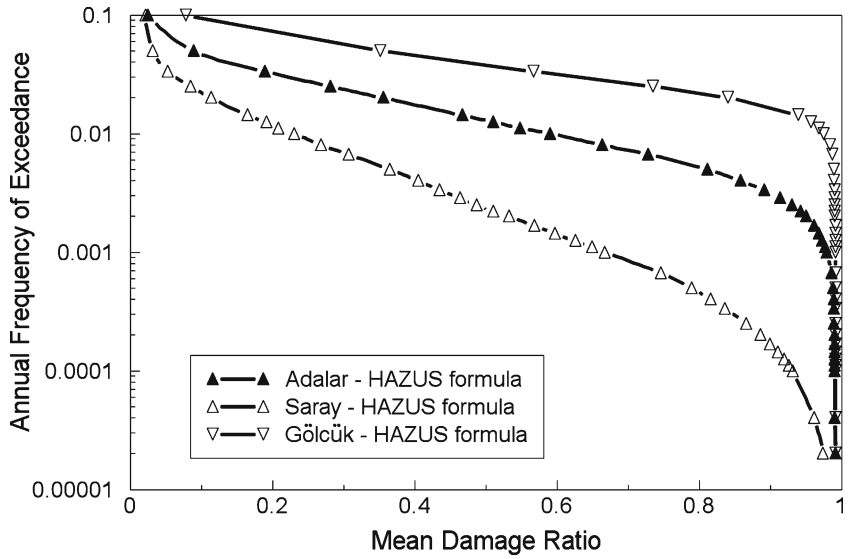

Figure 7. Loss exceedance curves for three municipalities in the Marmara region (note that the annual frequency of exceedance is the reciprocal of the return period).

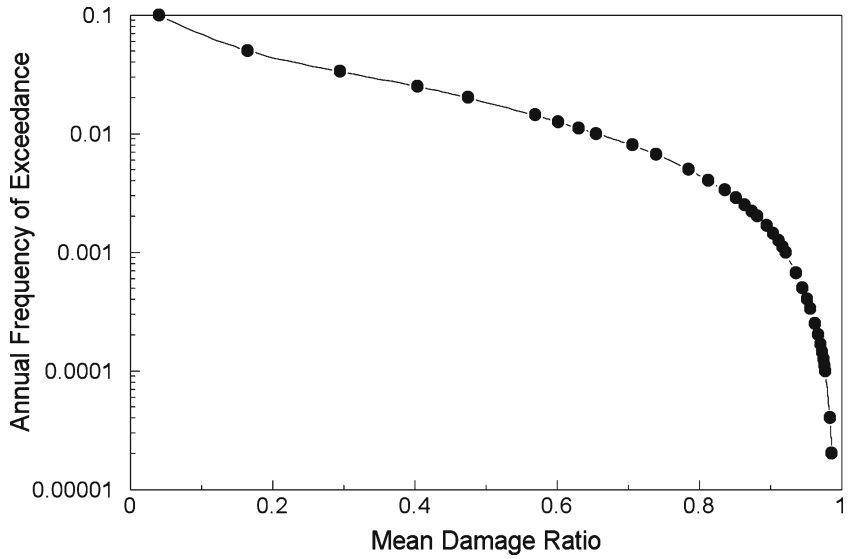

Figure 8. Combined loss exceedance curve for the three municipalities using mean damage ratio (MDR) formula suggested in HAZUS (FEMA, 2003).

and 100% for complete damage. The combined loss exceedance curve, considering the losses at all three sites, is presented in Figure 8.

By observing Figure 7 it is apparent that a large number of return periods (the reciprocal of the AFOE) is indeed required between 10 and

100 years (AFOE = 0.1–0.01) in the Marmara region due to the high seismic activity and vulnerability of the structures; in fact return periods even lower than 10 years appear to be required at Gölcük. Also, it would not have been correct to place a cap of 2500 years (AFOE = 0.0004) on the return period, as suggested in FEMA 366, as the mean damage ratio does increase at Saray for higher return periods. However, these loss curves are only illustrative as the current version of DBELA does not account for the influence of infill panels on the non-linear response of reinforced concrete frames, though it is well known that these exert a significant influence. Thus, this may explain why the loss estimates presented in Figure 7 appear to be very high, especially at Gölcük where it is predicted that all of the building stock is completely damaged every 100 years (AFOE = 0.01) on average. Additional factors may also have caused such high estimates to be made: Gölcük is only 1.2 and 9 km away from two fault segments (S3 and S4) with characteristic magnitude earthquakes of 7.2 (M_w) and recurrence intervals of 140 years. In addition, the soil conditions at this site have been assumed to be stiff soil, which has an assumed shear wave velocity of just 250 m/s^2, hence the ground motion is highly amplified. Furthermore, the vulnerability of the building stock has been calculated using geometric and material properties that are assumed to be typical of the building stock in the region; however the vulnerability predicted using DBELA has been found by Crowley *et al.* (2005) to be highly sensitive to the definition of the capacity parameters and so real statistics of the building stock would need to be obtained in order to obtain reliable vulnerability estimates. Nevertheless, the aforementioned factors do not affect the conclusions of this study as the results presented herein are only for comparative and illustrative purposes and are not to be taken as loss model results for the Marmara region.

3.2. STOCHASTIC CATALOGUE-BASED LOSS CALCULATIONS

Once a catalogue of scenarios using MCS has been generated and random ground motions at each site for each event have been sampled (see Section 2.5), then combined loss exceedance curves are calculated as follows:

(i) For each earthquake event, displacement spectra at each site are produced using the predicted ground motions and these are convolved with the capacity to calculate the probability of failing each of the three limit states and thus the proportion of buildings in each damage band.
(ii) The MDR at each site is calculated and these are summed together for each event to give a total value of the loss for that event.
(iii) The procedure is repeated for each earthquake in the catalogue and then the list of total MDR values is sorted in order of size and when,

for example, 100,000 years of data have been generated, the MDR with a 10^{-3} annual probability of being exceeded can be found by picking the value, which is exceeded 100 times in 100,000 years, i.e. the 101st value in the sorted list. Each value of MDR is plotted against its AFOE to give a loss or MDR exceedance curve.

Loss exceedance curves have been produced for each of the three sites using the ground motions predicted at each site from the MCS of the 100,000 and 500,000 years earthquake catalogues, as presented in Figures 9 and 10, respectively. These curves are compared with those attained in Figure 7 using the FEMA 366 procedure and it can be observed that the two procedures produce very similar results owing to the similarity of the hazard curves, and any differences can be attributed to the limited number of simulations in the Monte–Carlo method, though these appear to be negligible. Differences could arise in the two curves by considering the influence of the magnitude of each scenario earthquake on the corner period of the response spectrum, though Crowley *et al.* (2005) have found that for this particular region the results were not particularly sensitive to the change in corner period. The additional computational effort of calculating the losses from a catalogue of 500,000 years does not appear to be cost-effective for this loss model. However, a different loss model with lower seismic hazard levels or lower vulnerability of the buildings may need the calculations to

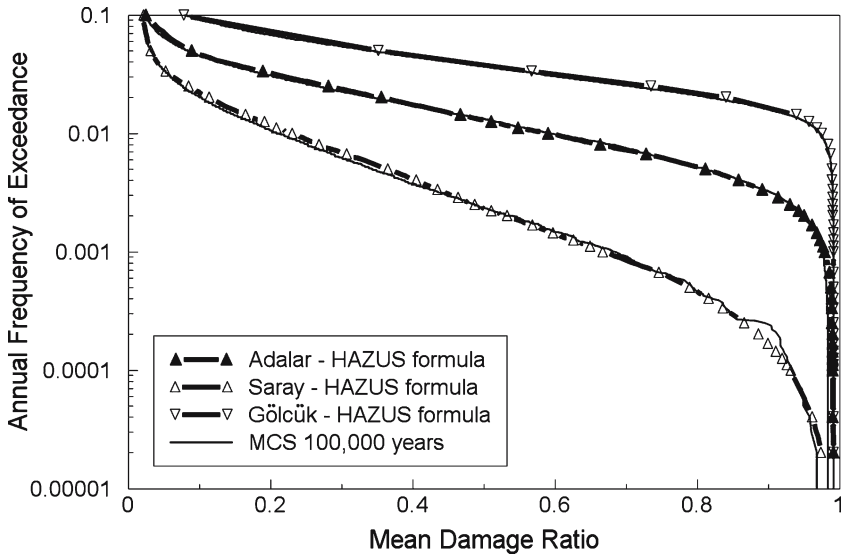

Figure 9. Comparison of loss exceedance curves for each of the three municipalities calculated using the FEMA 366 procedure (PSHA) with a procedure using a catalogue of earthquake scenarios spanning 100,000 yrs.

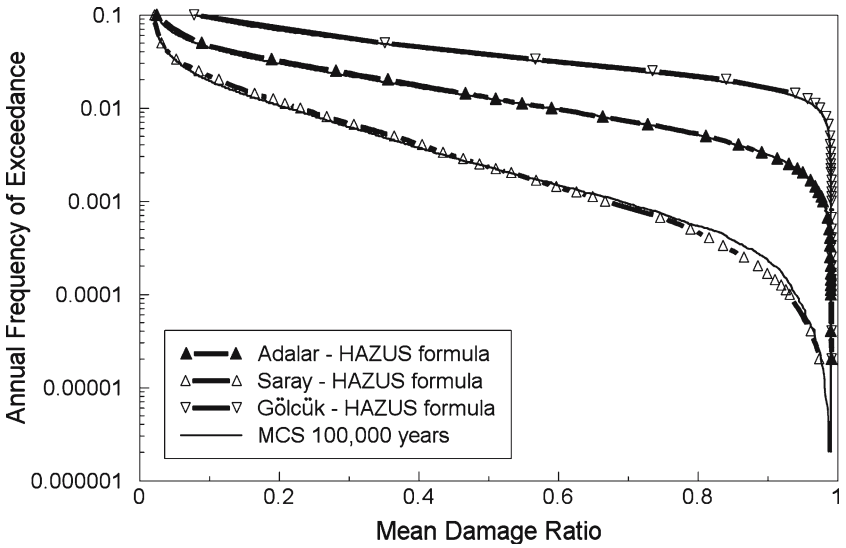

Figure 10. Comparison of loss exceedance curves for each of the three municipalities calculated using the FEMA 366 procedure (PSHA) with a procedure using a catalogue of earthquake scenarios spanning 500,000 yrs.

be carried out at even lower AFOE and in such cases it may be beneficial to use a longer earthquake catalogue.

To obtain combined loss exceedance curves for all three sites, the MDR estimated at each site from each scenario in the catalogue has been integrated and the resulting total MDR have been ordered in size and plotted against the number of times they are exceeded over the length of the catalogue (the AFOE). Figure 11 shows the combined loss exceedance curve using 100,000 years of seismicity along with that obtained with 500,000 years of seismicity. Again, the additional effort of using approximately five times more earthquake scenarios in the calculations is shown to be unwarranted.

3.3. COMPARISON OF LOSS CALCULATIONS

The combined loss exceedance curve obtained using the FEMA 366 procedure (see Figure 8) is compared in Figure 12 with the loss curve calculated using the multiple stochastic scenarios procedure (see Figure 11). There is a marked difference between the two curves with the former procedure leading to lower losses at high AFOE and higher losses at low AFOE. This figure confirms the fact that the seismic demand modelled by performing independent PSHA at several locations is effectively overestimated as a result of treating all of the ground-motion variability as being

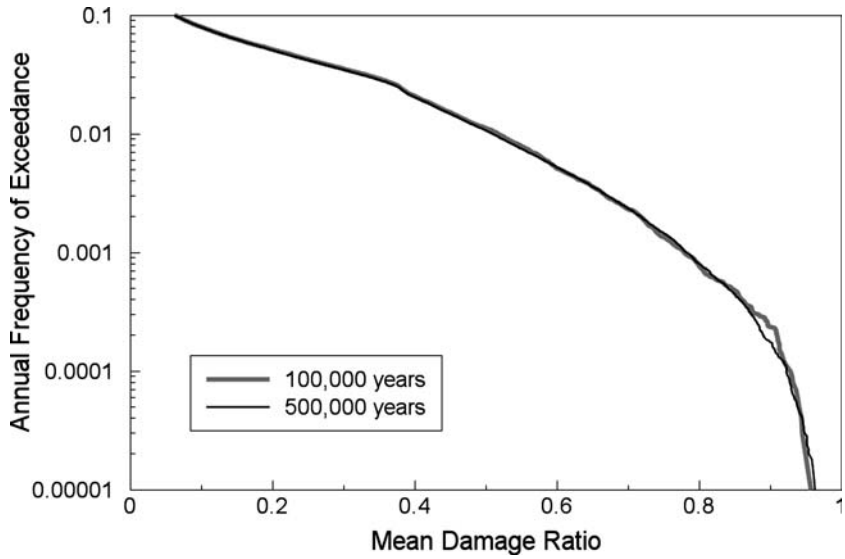

Figure 11. Combined loss exceedance curves for the three sites calculated using the scenarios from earthquake catalogues spanning 100,000 and 500,000 years.

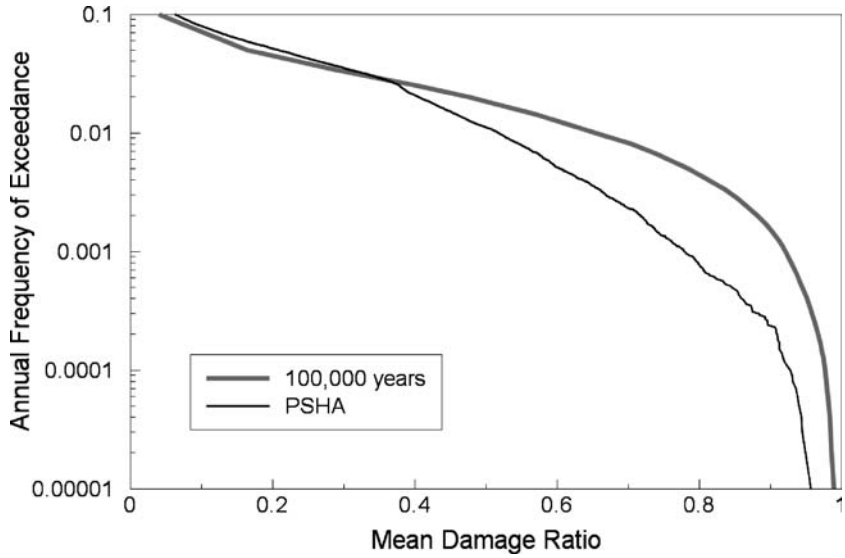

Figure 12. Comparison of loss exceedance curves obtained following the FEMA 366 procedure (PSHA) and through the use of multiple earthquake scenarios from a stochastic catalogue of 100,000 years length.

Table II. Comparison of AAL calculated for the two loss curves compared in Figure 12

Procedure	AAL (MDR)
FEMA 366	0.028
Stochastic catalogue 100,000 yrs	0.026

perfectly correlated inter-event (earthquake-to-earthquake) variability, whereas the main contributor to the scatter in ground-motion prediction equations is intra-event (spatial) variability (Bommer and Crowley, 2006). The importance of correctly modelling the correlation of the ground-motion field in loss models with spatially distributed exposure, and thus not treating the variability as being perfectly correlated, has also recently been noted by Wang and Takada (2005).

The AAL (in terms of MDR) has been calculated for the two loss curves in Figure 12 and the results are presented in Table II. The AAL obtained with the two procedures are very similar notwithstanding the differences in the loss curves. The AAL is controlled by the smaller and more frequent MDRs, whilst the higher MDRs are much less frequent and have a lower influence on the AAL. Therefore, considering the similarity of the two curves at higher AFOE, it is unsurprising that the two curves have similar AAL values. Similar conclusions have been obtained in other loss model studies (e.g. Bazzurro and Luco, 2005), wherein the modelling of the uncertainties and variability has been seen to have more influence on the loss exceedance curves than on the AAL values.

4. Discussion and conclusions

The aim of this paper has been to compare the results of a loss model using two different procedures to represent the seismic hazard: the use of conventional PSHA to obtain hazard curves at many locations, and the use of multiple earthquake scenarios, defined through MCS based on the seismicity model, to generate the ground motions at all sites of interest.

The two procedures have been seen to produce very different loss exceedance curves for a geographically distributed building stock, even though the same seismic hazard is represented in both methods. The differences in the estimated losses arise primarily from the way in which the aleatory variability in the ground-motion prediction equation is interpreted, as discussed by Bommer and Crowley (2006). Additional problems that arise with using PSHA as the basis for loss modelling are related to the fact that parameters such as earthquake magnitude are difficult to incorporate, which is relevant, for example, when the demand is dependent on

the duration of ground motion. Although outside the scope of this paper, this issue is equally relevant to loss models considering the impact of liquefaction (Bird *et al.*, 2006).

The use of the Monte–Carlo method to produce displacement spectra still requires further improvement because the calculation of the ordinates at each period using a randomly selected number of standard deviations requires the assumption that the ordinates are perfectly correlated, which is known not to be the case (Bazzurro and Cornell, 2002). Elements of the Vector-PSHA methodology of Bazzurro and Cornell (2002) could be followed to define correlation functions and combine these with the predictive models in the MCS so that a joint probability representation of the shaking, as opposed to an individual parameter characterisation, can be calculated.

The impact of correctly modelling the seismic hazard in loss assessment has been seen herein to be more evident in the loss exceedance curves than in the calculation of the AAL. Since the AAL is widely used in insurance applications, the penalty paid in terms of computational effort, when modelling the hazard through multiple earthquake scenarios may not always be justified, but it is clear that the use of PSHA should nonetheless be viewed as a compromise.

Acknowledgements

The authors would like to thank Professor Mustafa Erdik for providing data for the probabilistic seismic hazard assessment of the Marmara region (Turkey) and also to Shigeko Tabuchi and Oliver Peteken of Willis for providing building stock data for the same region. Selamet Yazici of the General Directorate of Insurance, the Prime Ministry, Turkey also deserves particular acknowledgement for authorising the use of the building stock data. The authors would also like to thank an anonymous reviewer for comments which helped to improve the manuscript. We are also grateful to many other individuals for input and discussions including Juliet Bird, Rui Pinho, Ihsan Engin Bal and Paolo Franchin.

References

Bazzurro, P. and Cornell, C.A. (1999) Disaggregation of seismic hazard. *Bulletin of the Seismological Society of America* **89**, 501–520.

Bazzurro, P. and Cornell, C.A. (2002) Vector-valued probabilistic seismic hazard analysis (VPSHA). *Proceedings of the 7th US National Conference on Earthquake Engineering*, Boston, MA, USA.

Bazzurro, P. and Luco, N. (2005) Accounting for uncertainty and correlation in earthquake loss estimation. *Proceedings of 9th International Conference on Structural Safety and Reliability (ICOSSAR '05)*, Rome, Italy.

Bird, J.F., Bommer, J.J., Crowley, H. and Pinho, R. (2006) Modelling liquefaction-induced building damage in earthquake loss estimation. *Soil Dynamics & Earthquake Engineering* **26**(1), 15–30.

Bommer, J.J. and Crowley, H. (2006) The influence of ground motion variability in earthquake loss modelling. *Bulletin of Earthquake Engineering, this volume*.

Bommer, J.J. and Mendis, R. (2005) Scaling of spectral displacement ordinates with damping ratios. *Earthquake Engineering and Structural Dynamics* **34**(2), 145–165.

Bommer, J.J., Pinho, R. and Crowley, H. (2005) Using displacement-based earthquake loss assessment in the selection of seismic code design levels. *Proceeding of ICOSSAR'05* (*International Conference on Structural Safety and Reliability*), Rome, 3567–3574.

Bommer, J.J., Spence, R., Erdik, M., Tabuchi, S., Aydinoglu, N., Booth, E., del Re, D. and Peterken, O. (2002) Development of an earthquake loss model for Turkish catastrophe insurance. *Journal of Seismology* **6**(3), 431–446.

Boore, D.M., Joyner, W.B. and Fumal, T.E. (1997) Equations for estimating horizontal response spectra and peak accelerations from western North American earthquakes: a summary of recent work. *Seismological Research Letters* **68**(1), 128–153.

Campbell, K.W., Thenhaus, P.C., Barnhard, T.P. and Hampson, D.B. (2000a) Seismic hazard model for loss estimation and risk management in the United States. *Proceedings of the 6th International Conference on Seismic Zonation*, Palm Springs, US.

Campbell, K.W., Thenhaus, P.C., Barnhard, T.P. and Hampson, D.B. (2000b) Seismic hazard model for loss estimation and risk management in Japan. *Proceedings of the 6th International Conference on Seismic Zonation*, Palm Springs, US.

Cao, T., Petersen, M.D., Cramer, C.H., Toppozada, T.R., Reichle, M.S. and Davis, J.F. (1999) The calculation of expected loss using probabilistic seismic hazard. *Bulletin of the Seismological Society of America* **89**(4), 867–876.

Cardona, O.M. and Yamin, L.E. (1997) Seismic microzonation and estimation of earthquake loss scenarios: integrated risk mitigation project of Bogotá, Colombia. *Earthquake Spectra* **13**(4), 795–814.

CEN (2003) Eurocode 8. Design of structures for earthquake resistance – Part 1: general rules seismic actions and rules for buildings. Pr. En 1998-1. Final draft, December 2003.

Chang, S.E., Shinozuka, M. and Moore, J.E. (2000) Probabilistic earthquake scenarios: extending risk analysis methodologies to spatially distributed systems. *Earthquake Spectra* **16**(3), 557–572.

Crowley, H., Pinho, R. and Bommer, J.J. (2004) A probabilistic displacement-based vulnerability assessment procedure for earthquake loss estimation. *Bulletin of Earthquake Engineering* **2**(2), 173–219

Crowley, H., Bommer, J.J., Pinho, R. and Bird, J. (2005) The impact of epistemic uncertainty on an earthquake loss model. *Earthquake Engineering and Structural Dynamics* **34**(14), 1663–1685.

Erdik, M., Demircioglu, M., Sesetyan, K., Durukal, E. and Siyahi, B. (2004) Earthquake hazard in Marmara region, Turkey. *Soil Dynamics and Earthquake Engineering* **24**, 605–631.

Ergun, M. and Ozel, E. (1995) Structural relationship between the Sea of Marmara basin and the North Anatolian Fault Zone. *Terra Nova* **7**, 278–288.

Eugster, S., Rüttener, E. and Liechti, D. (1999) The risk premium distribution (annual average loss) with respect to earthquake magnitude. *Proceedings of XXIV European Geophysical Society General Assembly*, The Hague, The Netherlands, 19–23 April, 1999.

Faccioli, E., Pessina, V., Calvi, G.M. and Borzi, B. (1999) A study on damage scenarios for residential buildings in Catania City. *Journal of Seismology* **3**, 327–343.

FEMA (2001) *FEMA 366: HAZUS Estimated Earthquake losses for the United States*.Federal Emergency Management Agency. Washington, DC.

FEMA (2003) *HAZUS-MH Technical Manual, Federal Emergency Management Agency*. Washington, DC.

FEMA (2004) *NEHRP Recommended Provisions for Seismic Regulations for New Buildings and Other Structures, 2003 Edition, Part 1 – Provisions, Part 2 – Commentary. FEMA 450*. Federal Emergency Management Agency. Washington, DC.

Leonard, G. and Steinberg, D.M. (2002) Seismic hazard assessment: simultaneous effect of earthquakes at close and distant sites. *Earthquake Spectra* **18**(4), 615–629.

Le Pichon, X, Taymaz, T. and Sengör, A.M.C. (1999) The Marmara fault and the future Istanbul earthquake. *International Conference on the Kocaeli earthquake, 17th August 1999, Istanbul*: Istanbul Technical University Press House, 41–54.

Liechti, D., Rüttener, E. and Zbinden, A. (2000) Disaggregation of average annual loss. *Presented at XXV European Geophysical Society General Assembly*, Nice, France, 25–29 April, 2000.

McGuire, R.K. (1995) Probabilistic seismic hazard analysis and design earthquakes: closing the loop. *Bulletin of the Seismological Society of America* **85**(5), 1275–1284.

Musson, R.M.W. (1998) On the use of Monte Carlo simulations for seismic hazard assessment. *Proceedings of 6th U.S. National Conference on Earthquake Engineering*. Seattle, Washington.

Musson, R.M.W. (1999) Determination of design earthquakes in seismic hazard analysis through Monte Carlo simulation. *Journal of Earthquake Engineering* **3**(4), 463–474.

Pinar, N. (1943) Marmara denizi havzasinin sismik jeolojisi ve meteorolojisi. *Science Faculty Monographies*, A7.

Rhoades, D.A. and McVerry, G.H. (2001) Joint hazard of earthquake shaking at two or more locations. *Earthquake Spectra* **17**(4), 697–710.

Risk Engineering Inc. (1998) EZ-FRISK™ Software for earthquake ground motion estimation. Version 4.1.

Spence, R., Bommer, J.J., Del Re, D., Bird, J., Aydinoglu, N. and Tabuchi, S. (2003) Comparing loss estimation with observed damage: a study of the 1999 Kocaeli earthquake in Turkey. *Bulletin of Earthquake Engineering* **1**(2), 83–113.

Tantala, M., Dargush, A., Deodatis, G., Jacob, K., Nordenson, G., O'Brien, D. and Swiren, B. (2002) Earthquake loss estimation for the New York City area. *Proceedings of the 7th U.S. National Conference on Earthquake Engineering*. Boston, MA, USA.

Taylor, C.E., Werner, S.D. and Jakubowski, S. (2001) Walkthrough method for catastrophe decision making. *Natural Hazards Review* **2**(4), 193–202.

Wang, M. and Takada, T. (2005) Macrospatial correlation model of seismic ground motions. *Earthquake Spectra* **21**(4), 1137–1156.

Wells, D.J. and Coppersmith, K.J. (1994) New empirical relationships among magnitude, rupture length, rupture width, rupture area, and surface displacement. *Bulletin of the Seismological Society of America* **84**, 974–1002.

Windeler, D., Morrow, G., Williams, C.R., Rahnama, M., Molas, G., Peña, A. and Bryngelson, J. (2004) Earthquake risk estimates for residential construction in the western United States. *Proceedings of 13th World Conference on Earthquake Engineering*. Vancouver, BC, Canada, August 1–6, 2004.

Zolfaghari, M.R. (2000) Earthquake loss estimation model for southern Europe. *Proceedings of 6th International Conference on Seismic Zonation*. Palm Springs, CA.